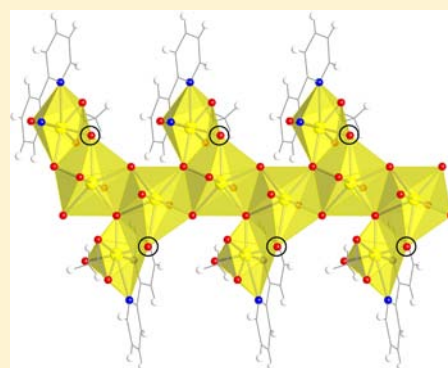


One-Dimensional Uranyl-2,2'-bipyridine Coordination Polymer with Cation–Cation Interactions:  $(\text{UO}_2)_2(2,2'\text{-bpy})(\text{CH}_3\text{CO}_2)(\text{O})(\text{OH})$ Pius O. Adelani<sup>†</sup> and Peter C. Burns<sup>\*,†,‡</sup><sup>†</sup>Department of Civil and Environmental Engineering and Earth Sciences and <sup>‡</sup>Department of Chemistry and Biochemistry, University of Notre Dame, Notre Dame, Indiana 46556, United States

## Supporting Information

**ABSTRACT:** A uranyl-2,2'-bipyridine coordination polymer,  $(\text{UO}_2)_2(2,2'\text{-bpy})(\text{CH}_3\text{CO}_2)(\text{O})(\text{OH})$  (**1**; 2,2'-bpy = 2,2'-bipyridine) has been synthesized hydrothermally at 165 °C and characterized via single-crystal X-ray diffraction and UV–vis–near-IR, fluorescence, and IR spectroscopies. The structure consists of two uranyl pentagonal bipyramids that are linked through cation–cation interactions (CCIs) to form chains that are truncated in the second and third dimensions by 2,2'-bpy. These chains of uranyl polyhedra consist of a rare case of CCIs through the edge-sharing polyhedral connection mode instead of the more common corner-sharing connection mode. **1** is the first uranium(VI) compound reported that contains CCIs in which the structural unit is one-dimensional, although lower-dimensional structural units with CCIs are known for pentavalent actinides.



## INTRODUCTION

Hybrid uranyl–organic materials combine the unique characteristics and properties of their organic components with uranyl units to produce significant diversity in structure, bonding, and application. This area of study has been widely investigated in recent years, and various organic substructures have been incorporated into inorganic oxides (i.e., carboxylate or phosphonate groups), leading to promising applications in the field of gas storage, ion exchange, intercalation chemistry, photochemistry, catalysis, etc.<sup>1</sup> In principle, traditional metal–organic coordination chemistry involves the synthesis of molecular species using terminal ligands, whereas divergent ligands are used to construct the extended network of the metal–organic coordination polymers or frameworks (three-dimensional). With this understanding, we developed our previous work that yielded a series of three-dimensional uranyl–organic frameworks using phosphonate ligands with rigid phenyl groups.<sup>1b,c,2</sup> In contrast to our previous results where we utilized a divergent ligand, we report here the design of a one-dimensional uranyl chain of  $(\text{UO}_2)_2(2,2'\text{-bpy})(\text{CH}_3\text{CO}_2)(\text{O})(\text{OH})$  (**1**) using 2,2'-bipyridine as a terminal ligand.

The solid-state coordination chemistry of uranium is largely dominated by  $\text{U}^{\text{VI}}$ , which exists as a uranyl cation, the  $\text{UO}_2^{2+}$  moiety.  $\text{U}^{\text{VI}}$  is flexible in its modes of coordination; the axial sites are occupied by two oxygen atoms, whereas the equatorial sites are coordinated by four to six ligands, giving tetragonal-, pentagonal-, and hexagonal-bipyramidal geometries. The “yl” oxygen atoms of the linear uranyl ion,  $[\text{O}=\text{U}=\text{O}]^{2+}$ , are typically unreactive and terminate bonding along the axial plane, resulting in the widely recognized two-dimensional sheets of uranyl polyhedra.<sup>3</sup> The two distinct uranyl sites of **1**

are linked via cation–cation interactions (CCIs), in which a uranyl “yl” oxygen atom of  $\text{U}^{\text{VI}}$  coordinates to the  $\text{U}^{\text{VI}}$  site at an equatorial position. CCIs are rare in compounds that exclusively contain  $\text{U}^{\text{VI}}$  and are much more common in pentavalent actinyl chemistry.<sup>4</sup> Nevertheless, uranyl cations often form interactions with alkali and alkali-earth metal cations in solid-state compounds.<sup>1b,c,2h</sup> The prevalence of CCIs is most recognized for  $\text{Np}^{\text{V}}$ , relative to the  $\text{UO}_2^{2+}$  cation and other actinyl compounds ( $\text{An}^{\text{V}} = \text{U}^{\text{V}}, \text{Pu}^{\text{V}}, \text{Am}^{\text{V}}$ ).<sup>4b,5</sup> The discrepancy between  $\text{U}^{\text{VI}}$  and  $\text{Np}^{\text{V}}$  is likely due to the differences in the Lewis basicity of their “yl” oxo ligands and the high stability of  $\text{Np}^{\text{V}}$  relative to other  $\text{An}^{\text{V}}$  cations, which are easily amenable to phenomena like disproportionation, oxidation, and reduction.<sup>4a</sup> Despite their rarity, a handful of CCIs have been observed in the solid-state for  $\text{U}^{\text{VI}}$ , including a few examples that have been described in uranyl–organic compounds<sup>6</sup> as well as in purely inorganic complexes.<sup>7</sup>

In this contribution, we describe the synthesis of a hybrid uranyl–organic coordination polymer that exhibits CCIs in a one-dimensional infinite chain, structural characterization from single-crystal X-ray diffraction (XRD), and spectroscopic data.

## EXPERIMENTAL SECTION

**Synthesis.**  $\text{UO}_2(\text{CH}_3\text{COO})_2 \cdot 2\text{H}_2\text{O}$  (98%, Alfa-Aesar), 2,2'-bipyridine (2,2'-bpy; 98%, Alfa-Aesar), hydrofluoric acid (HF; 48 wt %, Aldrich), and (4-aminophenyl)arsonic acid (98%, Aldrich) were used as received. Reactions were conducted in poly(tetrafluoroethylene)-lined Parr 4749 autoclaves with a 23 mL internal volume. Distilled and Millipore-filtered water with a resistance of 18.2  $\text{M}\Omega\text{-cm}$  was used in

Received: August 14, 2012

Published: September 24, 2012

all reactions. **Caution!** While the uranium compound used in these studies contained depleted uranium, precautions are needed for handling radioactive materials, and all studies should be conducted in a laboratory dedicated to studies of radioactive materials.

**(UO<sub>2</sub>)<sub>2</sub>(2,2'-bpy)(CH<sub>3</sub>CO<sub>2</sub>)<sub>2</sub>(O)(OH) (1).** UO<sub>2</sub>(CH<sub>3</sub>COO)<sub>2</sub>·2H<sub>2</sub>O (354.5 mg, 8.4 mmol), (4-aminophenyl)arsonic acid (90.4 mg, 4.2 mmol), 2,2'-bpy (52.0 mg, 3.3 mmol), 3.0 mL of water, and HF (~15 μL, 0.4 mmol) were loaded into a 23 mL autoclave. The autoclave was sealed and heated to 165 °C in a box furnace for 3 days. The autoclave was then cooled at an average rate of 5 °C h<sup>-1</sup> to 25 °C. The resulting yellow product was washed with distilled water and methanol and allowed to air-dry at room temperature. Yellow crystals of **1** suitable for XRD studies were formed along with powder. The brown powder was the major product, and the crystals of **1** formed about 40% of the products.

**Crystallographic Studies.** A single crystal of **1** was mounted on a glass fiber with epoxy and optically aligned on a Bruker APEX CCD X-ray diffractometer using a digital camera. Initial intensity measurements were performed using graphite-monochromated Mo K $\alpha$  radiation ( $\lambda = 0.71073$  Å) from a conventional sealed tube and a monochromator. SMART (version 5.624) was used for the preliminary determination of the cell constants and data collection control. The intensities of the reflections of a sphere were collected by a combination of three sets of exposures (frames). Each set had a different  $\varphi$  angle for the crystal, and each exposure covered a range of 0.5° in  $\omega$ . A total of 1464 frames were collected with an exposure time per frame of 30 s. SAINT software was used for data integration including Lorentz and polarization corrections. A semiempirical absorption correction was applied using the program SADABS.<sup>8</sup> The program suite SHELXTL was used for space-group determination (XPREF), direct method structure solution (XS), and least-squares refinement (XL).<sup>9</sup> The positions of the hydrogen atoms around the carbon atoms were included using a riding model. The final refinement included anisotropic displacement parameters for all atoms except hydrogen. Select crystallographic information is listed in Tables 1 and 2. Atomic coordinates, bond distances, and additional structural information are provided in the Supporting Information.

**Table 1. Crystallographic Data for 1**

compound	<b>1</b>
fw	787.29
color and habit	yellow, acicular
space group	<i>P</i> <sub>2</sub> <sub>1</sub> / <i>c</i>
<i>a</i> (Å)	10.6289(7)
<i>b</i> (Å)	7.4233(5)
<i>c</i> (Å)	20.4411(13)
$\beta$ (deg)	96.686(1)
<i>V</i> (Å <sup>3</sup> )	1601.86(18)
<i>Z</i>	4
<i>T</i> (K)	193
$\lambda$ (Å)	0.71073
$\rho_{\text{calcd}}$ (g cm <sup>-3</sup> )	3.265
$\mu$ (Mo K $\alpha$ ) (mm <sup>-1</sup> )	20.24
<i>R</i> ( <i>F</i> ) for $F_o^2 > 2\sigma(F_o^2)^a$	0.030
$wR(F_o^2)^b$	0.061

<sup>a</sup> $R(F) = \frac{\sum ||F_o| - |F_c||}{\sum |F_o|}$ . <sup>b</sup> $R(F_o^2) = \frac{\sum w(F_o^2 - F_c^2)^2}{\sum wR(F_o^4)^{1/2}}$ .

**Powder XRD.** A powder XRD pattern of compound **1** was collected on a Bruker  $\theta$ - $\theta$  diffractometer equipped with a Lynxeye one-dimensional solid-state detector and Cu K $\alpha$  radiation at room temperature over the angular range from 5° to 60° (2 $\theta$ ) with a scanning step width of 0.02° and a fixed counting time of 15 s step<sup>-1</sup>. The powder pattern from the bulk powder and crystals of **1** is compared with the simulated powder pattern from the single-crystal data of **1** in the Supporting Information.

**Table 2. Selected Interatomic Distances (Å) and Angles (deg) for 1**

Distances (Å)			
U1–O1	1.790(4)	U2–O5	2.380(4)
U1–O6	1.820(4)	U2–O6	2.571(4)
U1–O5	2.118(4)	U2–U2 <sup>i</sup>	3.8135(3)
U1–O7	2.404(5)	O8–C11	1.272(8)
U1–O8	2.444(5)	O7–C11	1.260(9)
U1–N1	2.562(5)	C11–C12	1.488(10)
U1–N2	2.603(6)	N1–C1	1.345(9)
U1–U2	3.5930(3)	N1–C5	1.349(9)
U2–O4	1.769(4)	N2–C6	1.354(9)
U2–O3	1.778(4)	N2–C10	1.353(9)
U2–O5 <sup>i</sup>	2.305(4)	C5–C4	1.378(10)
U2–O2	2.319(4)	C5–C6	1.477(9)
U2–O2 <sup>i</sup>	2.345(4)		
Angles (deg)			
O1–U1–O6	177.8(2)	O3–U2–O4	178.2(2)

**Spectroscopic Properties.** Absorption and fluorescence data for **1** were acquired from a single crystal using a Craic Technologies UV–vis–near-IR (NIR) microspectrophotometer with a fluorescence attachment. The absorption data were collected in the range of 250–1200 nm at room temperature. Excitation was achieved using 365 nm light from a mercury lamp for the fluorescence spectroscopy. The IR spectrum was collected from a single crystal of **1** using a SensIR Technology IlluminatIR FT-IR microspectrometer. A single crystal of **1** was placed on a glass slide, and the spectrum was collected with a diamond ATR objective.

## RESULTS AND DISCUSSION

**Synthesis.** The addition of HF to the reactants is essential; it serves as a mineralizing agent in the synthesis, and its absence resulted in the isolation of powders as the only products. We isolated a uranyl-2,2'-bipyridine coordination polymer without CCI interactions when we attempted the synthesis without (4-aminophenyl)arsonic acid. The (4-aminophenyl)arsonic acid used in this synthesis may be acting as a buffer in the reaction, and it decomposes at higher temperature. The powder XRD pattern collected for the products indicates the presence of **1**, minor U<sub>3</sub>O<sub>8</sub>, and one or more phases that could not be identified (Supporting Information).

**Structure of 1.** The structure of **1** adopts monoclinic space group *P*<sub>2</sub><sub>1</sub>/*n* and consists of two crystallographically distinct U<sup>VI</sup> centers that occur in pentagonal-bipyramidal coordination geometries. These uranyl bipyramids share edges through the oxide ligand and CCIs, as shown in Figure 1. The overall structure contains chains built from the uranyl pentagonal bipyramids (see Figures 2 and 3). This is in contrast to all reported uranyl(VI) compounds that contain CCIs, which have framework structures.<sup>6,7</sup> However, lower-dimensional structures with CCIs are common for neptunyl(V) compounds<sup>4g–m</sup> and have been reported for U<sup>V,5m,n</sup>. In **1**, the chains of uranyl polyhedra extend along [010], whereas the converging ligand, 2,2'-bpy, prevents linkage to uranyl polyhedra in the other dimensions. The uranyl chains are connected by hydrogen-bonding interactions via the acetate and 2,2'-bpy moieties, H<sub>2</sub>C<sub>acetate</sub>–H $\cdots$ O=U (2.544–2.672 Å) and C<sub>2,2'-bpy</sub>–H $\cdots$ O=U (2.444–2.722 Å) (Figure 4).

Several examples of uranyl(V) complexes with CCIs have been reported by the Mazzanti and Boncella groups.<sup>4g–m</sup> In contrast to **1**, these molecular structures assumed diamond-shaped dimeric,<sup>4d,h,i</sup> triangular-shaped trimeric,<sup>4m</sup> T-shaped

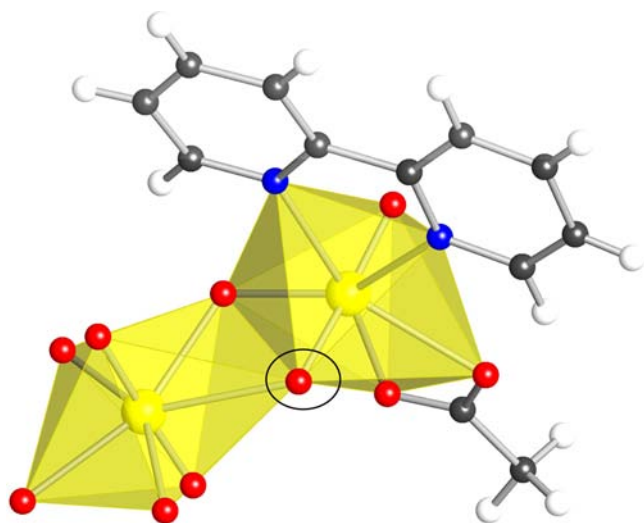


**Figure 1.** Illustration of the coordination environments of the two uranyl centers giving the CCI (black oval shape) in **1**. Color code: uranyl units, yellow; nitrogen, blue; oxygen, red; carbon, light black; hydrogen, white.

tetrameric,<sup>4g-k</sup> and linear-shaped tetrameric,<sup>4l</sup> complexes of CCIs (Figure 5). Boncella et al. reported an imido variant of the diamond-shaped dimer of the uranyl(V) complex with CCIs.<sup>4d</sup> The bulky ligands used to stabilize the  $\text{UO}_2^{2+}$  complexes truncate the extension of the uranyl chains instead of the common increase in the dimensionality of the uranyl polyhedra expected in complexes with CCIs.

The two distinct uranyl ions U1 and U2 have nearly linear  $[\text{O}=\text{U}=\text{O}]^{2+}$  bond angles of  $177.8(2)$  and  $178.2(2)^\circ$ , respectively. The four  $\text{U}=\text{O}$  bond distances are  $1.790(4)$ ,  $1.820(4)$ ,  $1.769(4)$ , and  $1.778(4)$  Å for U1–O1, U1–O6, U2–O4, and U2–O3, respectively. The bond length of O6 is noticeably longer, consistent with the weakening of the “yl”

oxygen atom that is shared with another uranyl center via a CCI ( $\mu_2$ -oxo-bridging oxygen atom). The uranyl cations are coordinated by five ligands in the equatorial planes of pentagonal bipyramids, consisting of nitrogen and/or oxygen atoms. The U1 center is coordinated by  $\text{O}_3\text{N}_2$  in the pentagonal plane, with the U1–O bond distances ranging from  $2.118(4)$  to  $2.444(5)$  Å and two U1–N bond distances of  $2.562(5)$  and  $2.603(6)$  Å. U2 is coordinated by five oxygen atoms, and the U2–O bond distances range from  $2.305(4)$  to  $2.571(4)$  Å. The distance between the uranium centers connected via the  $\mu_3$ -bridging oxo and  $\mu_2$ -bridging “yl” oxo atoms, U1–U2, is  $3.5930(3)$  Å in this inorganic motif. The sharing of edges between pentagonal bipyramids via  $\mu_2$ -hydroxo and  $\mu_3$ -oxo atoms bridge U2 sites, propagating along the infinite chain with a longer U–U distance of  $3.8135(3)$  Å. These U–U distances are notably shorter than most reported in other uranyl(VI) compounds.<sup>6a,b,7a</sup> We calculated bond-valence sums of 6.10 and 6.09 for U1 and U2, respectively, consistent with the assigned oxidation state of  $\text{U}^{\text{VI}}$ .<sup>10</sup> The bond valence for O6 is 1.56, and the values range from 1.65 to 1.72 for the other three “yl” oxo atoms. The value is expected to be less for an “yl” oxo atom that is involved in CCIs.

**Spectroscopic Properties.** UV–vis–NIR absorption spectroscopy has proven to be a useful diagnostic tool for demystifying uranium complexes in their various oxidation states (4+, 5+, and 6+). The absorption spectrum shown in Figure S2 in the Supporting Information reveals the characteristic equatorial U–O charge-transfer bands of uranyl centered at 330 nm, and the axial  $\text{U}=\text{O}$  charge-transfer bands were also observed along with characteristic fine structure for the 430 nm peak for  $\text{U}^{\text{VI}}$ .

The majority of uranyl compounds emit green light centered near 520 nm with strong vibronic coupling, yielding a well-resolved five-peak pattern.<sup>11</sup> However, not all uranyl compounds fluoresce, and the mechanisms of the emission are often difficult to explain. Despite the quenching character of CCIs,

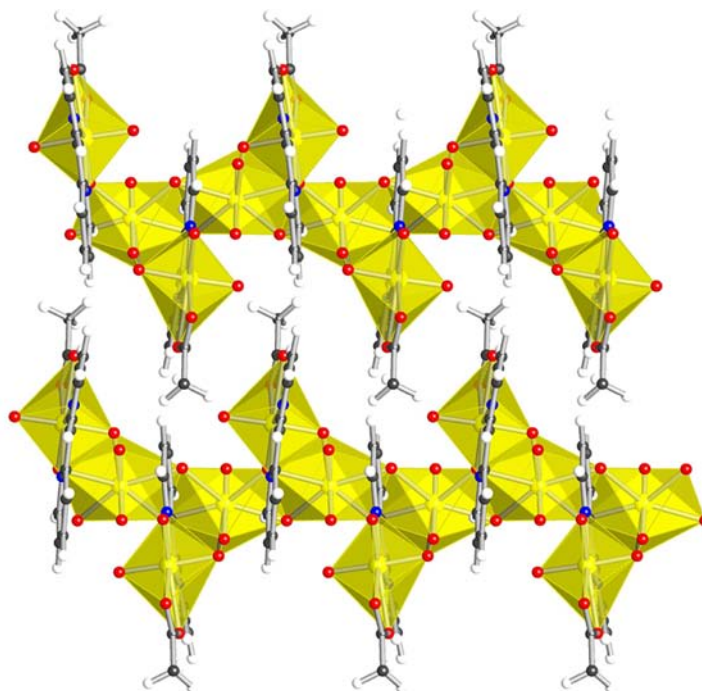


**Figure 2.** Polyhedral representation of the overall one-dimensional structure of **1**. Legend as in Figure 1.



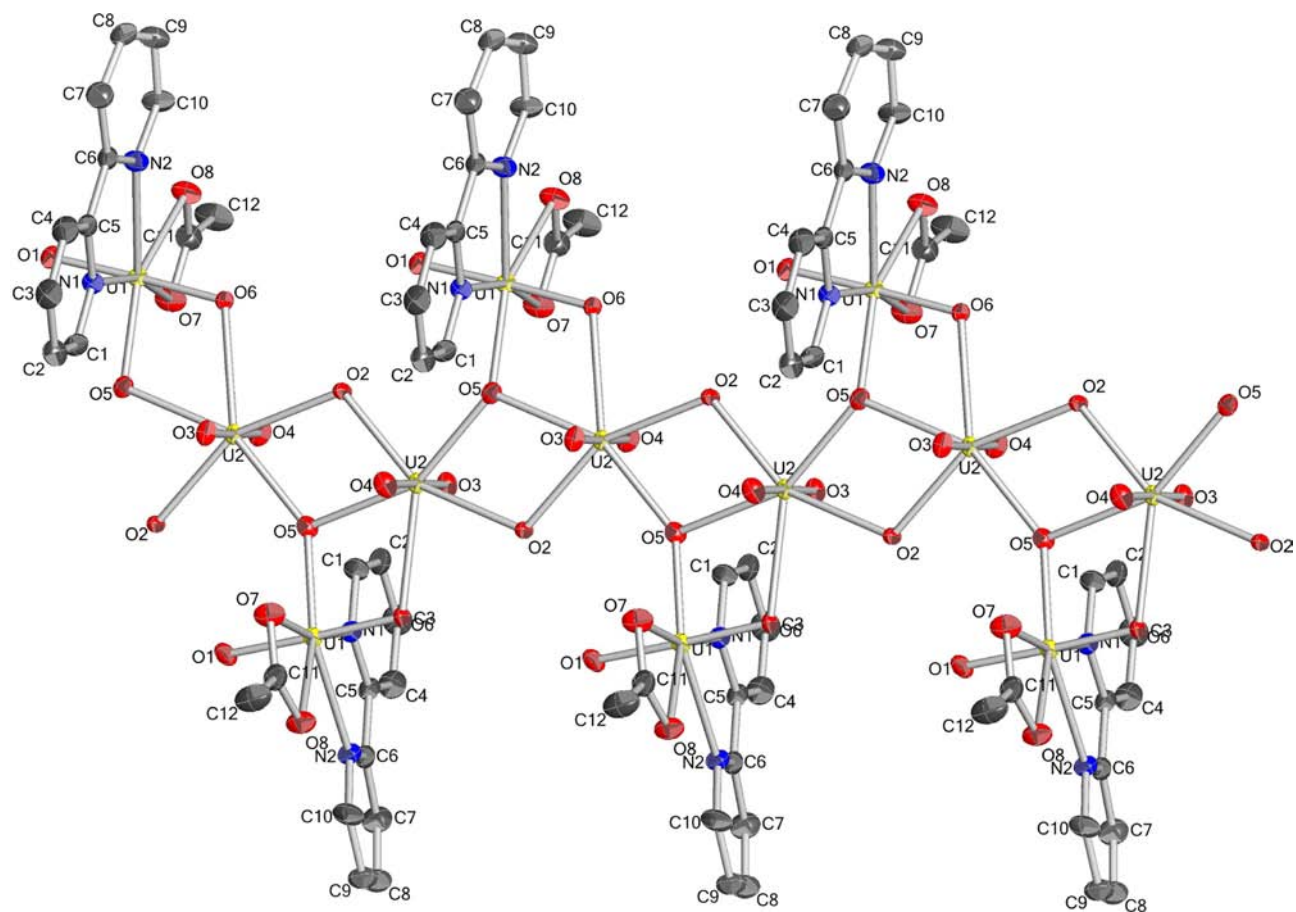


**Figure 3.** Depiction of the local coordination environment of the uranyl chain in **1**. Hydrogen atoms are omitted for clarity. Displacement ellipsoids are drawn at the 50% probability level.

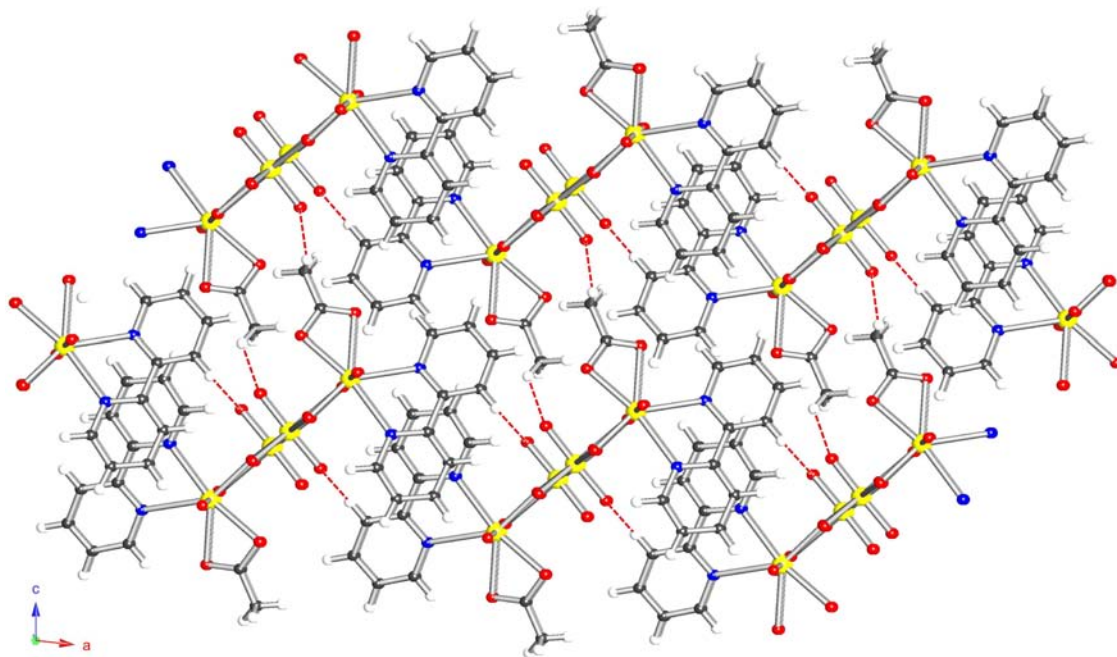


**Figure 4.** View of the hydrogen-bonding interactions between the acetate or 2,2'-bpy moieties and the linear uranyl dications in **1**.

$(\text{UO}_2)_8\text{O}_2(\text{OH})_4(\text{H}_2\text{O})_4(1,3\text{-bdc})_4 \cdot 4\text{H}_2\text{O}$ <sup>7b</sup> and  $\text{UO}_2(\text{NO}_2\text{TA})_2(\text{H}_2\text{O})$ <sup>7c</sup> (1,3-bdc = 1,3-benzenedicarboxylate;  $\text{NO}_2\text{TA}$  = 2-nitroterephthalic acid) fluoresce at room temper-

ature, while  $(\text{UO}_2)_2[\text{UO}_4(\text{trz})_2](\text{OH})_2$  (trz = 1,2,4-triazole) does not.<sup>7a</sup> In contrast,  $\text{Th}^{\text{IV}}$  has a  $5f^0$  configuration and emissions are not allowed, but we have reported luminescent

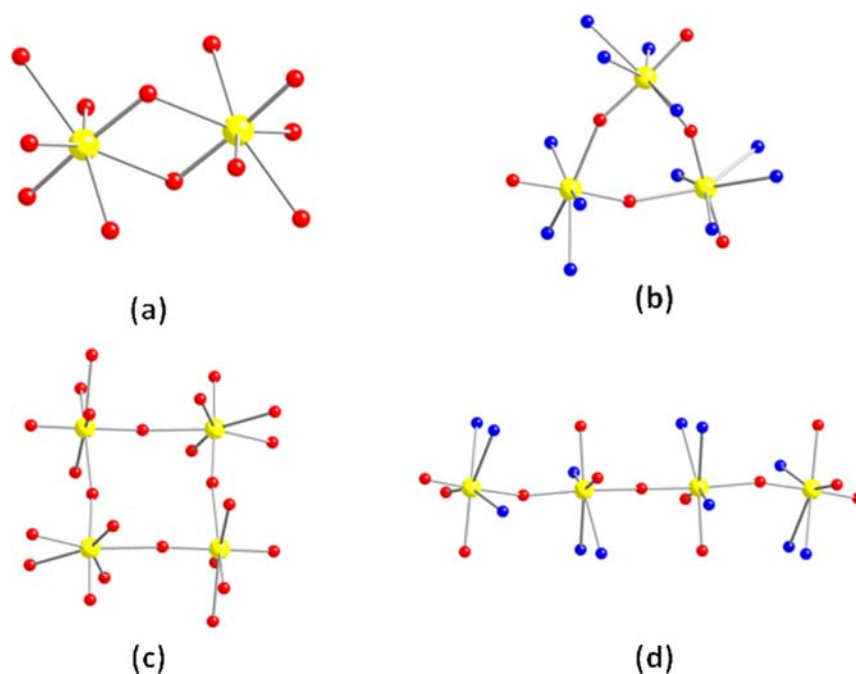


**Figure 5.** Geometries of the CCIs in  $U^V$  uranyl molecular structures: (a) diamond-shaped dimer; (b) triangular-shaped trimer; (c) T-shaped tetramer; (d) linear-shaped tetramer.

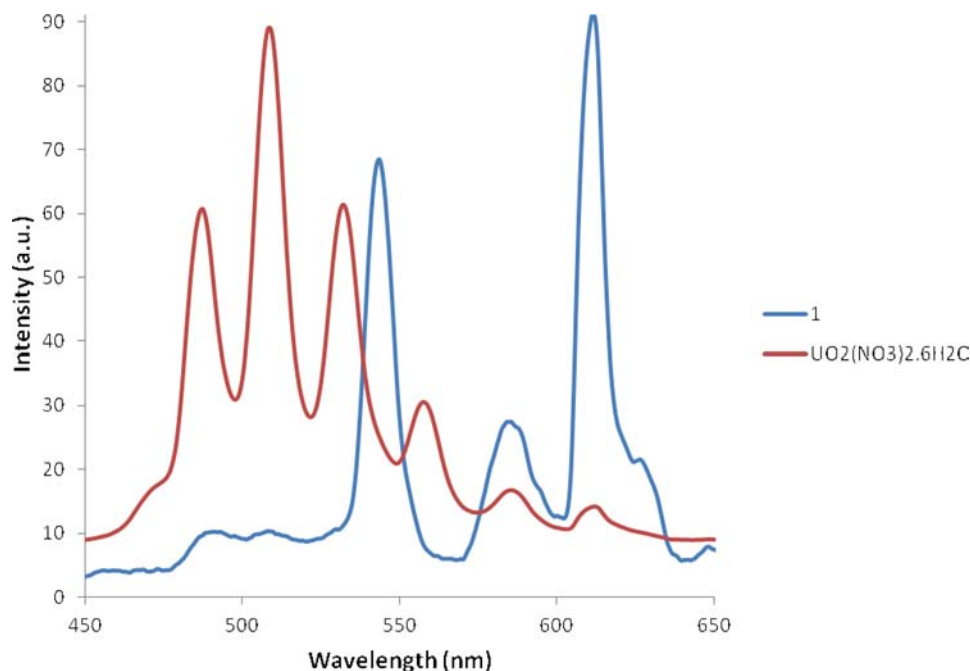


**Figure 6.** Fluorescence spectra of **1** and uranyl nitrate showing clearly resolved vibronically coupled charge-transfer transitions.

properties in  $\text{ThF}_2(\text{PO}_3\text{C}_6\text{H}_4\text{CO}_2\text{H})$ .<sup>12</sup> The fluorescence spectrum for **1** excited at 365 nm reveals the characteristic five-band emission pattern for uranyl compounds; peaks are resolved at 489, 508, 543, 584, and 611 nm (Figure 6). The most intense peak is positioned at 611 nm, which is red-shifted by approximately 108 nm relative to the corresponding five-band emission pattern in the spectrum of  $\text{UO}_2(\text{NO}_3)_2 \cdot 6\text{H}_2\text{O}$ . The slight difference can be ascribed to the influence of the coordinated 2,2'-bpy ligand.

The low-wavenumber regions of the IR spectrum (Figure 7), 683–775  $\text{cm}^{-1}$ , consist of peaks indicative of the ring

deformation of 2,2'-bpy, and the symmetric and asymmetric stretching modes of the uranyl cation,  $\text{UO}_2^{2+}$ , are positioned at 859 and 897  $\text{cm}^{-1}$ , respectively. Those bands from 1023 to 1250  $\text{cm}^{-1}$  are assigned to C–C stretches, C–H bending, and  $\text{CH}_3$  vibrations. The O–C–O symmetric stretches of the bound acetate is positioned at 1327  $\text{cm}^{-1}$ , while the bands for C=C and O–C–O antisymmetric stretches of the 2,2'-bpy and acetate, respectively, range from 1411 to 1501  $\text{cm}^{-1}$ . The C=N stretches of 2,2'-bpy are assigned to the bands from 1582 to 1605  $\text{cm}^{-1}$ . The high-energy regions (2944–3134  $\text{cm}^{-1}$ ) are dominated by the  $\text{CH}_3$  stretching of the acetate and

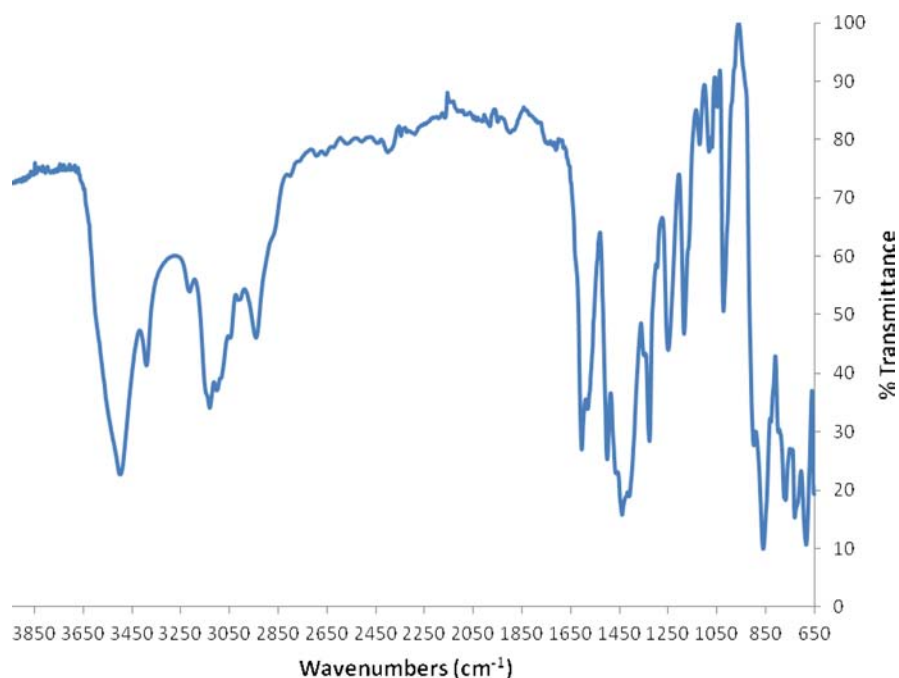


Figure 7. IR spectrum of the uranium compound **1**.

the C–H stretches of the 2,2'-bpy. The peaks at 3394 and 3502  $\text{cm}^{-1}$  are assigned to the O–H stretches of the hydroxide.<sup>1c,2c,13</sup>

## CONCLUSIONS

In conclusion, the synthesis of a one-dimensional uranyl-2,2'-bipyridine containing CCIs was achieved under mild hydrothermal conditions in the presence of (4-aminophenyl)arsonic acid. The structure of **1** differs from other widely known solid-state structures with CCIs, where these bonding behaviors serve to increase the dimensionality. The uranyl chains are terminated from extending in other directions by the use of 2,2'-bpy. This structure also differs from complexes of cation–cation  $\text{U}^{\text{V}}$  uranyl that are mostly molecular structures. **1** consists of a rare case of a CCI through the edge-sharing polyhedral connection mode instead of the more common corner-sharing connection mode.<sup>6b,7b,c</sup> However, the central issue that will be addressed by ongoing studies is the comparison of the coordination chemistry of uranium with arsonates and phosphonates.

## ASSOCIATED CONTENT

### Supporting Information

Absorption spectrum, powder XRD pattern, and crystallographic data in CIF format for compound **1**. This material is available free of charge via the Internet at <http://pubs.acs.org>.

## AUTHOR INFORMATION

### Corresponding Author

\*E-mail: [pburns@nd.edu](mailto:pburns@nd.edu).

### Notes

The authors declare no competing financial interest.

## ACKNOWLEDGMENTS

This material was supported by the Chemical Sciences, Geosciences and Biosciences Division, Office of Basic Energy Sciences, Office of Science, U.S. Department of Energy (Grant DE-FG02-07ER15880).

## REFERENCES

- (a) Alsobrook, A. N.; Hauser, B. G.; Hupp, J. T.; Alekseev, E. V.; Depmeier, W.; Albrecht-Schmitt, T. E. *Chem. Commun.* **2010**, 46, 9167. (b) Adelani, P. O.; Albrecht-Schmitt, T. E. *Angew. Chem., Int. Ed.* **2010**, 49, 8909. (c) Adelani, P. O.; Albrecht-Schmitt, T. E. *Inorg. Chem.* **2011**, 50, 12184. (d) Clearfield, A. *Prog. Inorg. Chem.* **1998**, 47, 371. (e) Cahill, C. L.; de Lill, D. T.; Frisch, M. *CrystEngComm* **2007**, 9, 15. (f) Frisch, M.; Cahill, C. L. *Dalton Trans.* **2006**, 39, 4679. (g) Clearfield, A. *Curr. Opin. Solid State Mater. Sci.* **2003**, 6, 495. (h) Cahill, C. L.; Borkowski, L. A. In *Structural and Chemistry of Inorganic Actinide Compounds*; Krivovichev, S. V., Burns, P. C., Tananaev, I. G., Eds.; Elsevier: Oxford, U.K., 2007; Chapter 11. (i) Knope, K. E.; Cahill, C. L. In *Metal Phosphonate Chemistry from Synthesis to Applications*; Clearfield, A., Demadis, K., Eds.; The Royal Society of Chemistry: London, 2012; Chapter 18.
- (a) Adelani, P. O.; Oliver, A. G.; Albrecht-Schmitt, T. E. *Cryst. Growth Des.* **2011**, 11, 1966. (b) Adelani, P. O.; Albrecht-Schmitt, T. E. *Inorg. Chem.* **2009**, 48, 2732. (c) Adelani, P. O.; Albrecht-Schmitt, T. E. *Cryst. Growth Des.* **2011**, 11, 4227. (d) Adelani, P. O.; Oliver, A. G.; Albrecht-Schmitt, T. E. *Cryst. Growth Des.* **2011**, 11, 3072. (e) Adelani, P. O.; Albrecht-Schmitt, T. E. *J. Solid State Chem.* **2011**, 184, 2368.
- (a) Burns, P. C.; Miller, M. L.; Ewing, R. C. *Can. Mineral.* **1996**, 34, 845. (b) Burns, P. C. *Can. Mineral.* **2005**, 43, 1839.
- (a) Fortier, S.; Hayton, T. W. *Coord. Chem. Rev.* **2010**, 254, 197. (b) Krot, N. N.; Grigoriev, M. S. *Russ. Chem. Rev.* **2004**, 73, 89. (c) Arnold, P. L.; Love, J. B.; Patel, D. *Coord. Chem. Rev.* **2009**, 253, 1973. (d) Spencer, L. P.; Schelter, E. J.; Yang, P.; Gdula, R. L.; Scott, B. L.; Thompson, J. D.; Kiplinger, J. L.; Batista, E. R.; Boncella, J. M. *Angew. Chem., Int. Ed.* **2009**, 48, 3795. (e) Guillaume, B.; Hobart, D. E.; Bourges, J. Y. *J. Inorg. Nucl. Chem.* **1981**, 43, 3295. (f) Stoyer, N. J.; Hoffman, D. C.; Silva, R. J. *Radiochim. Acta* **2000**, 88, 279. (g) Burdet, F.; Pecaut, J.; Mazzanti, M. *J. Am. Chem. Soc.* **2006**, 128, 16512. (h) Nocton, G.; Horeglad, P.; Pecaut, J.; Mazzanti, M. *J. Am. Chem. Soc.* **2008**, 130, 16633. (i) Graves, C. R.; Kiplinger, J. L. *Chem. Commun.* **2009**, 3831. (j) Mougél, V.; Horeglad, P.; Nocton, G.; Pécaut, J.; Mazzanti, M. *Angew. Chem., Int. Ed.* **2009**, 48, 8477. (k) Mougél, V.; Horeglad, P.; Nocton, G.; Pecaut, J.; Mazzanti, M. *Chem.—Eur. J.* **2010**, 16, 14365. (l) Mougél, V.; Pecaut, J.; Mazzanti, M. *Chem. Commun.* **2012**, 48, 868. (m) Chatelain, L.; Mougél, V.; Pecaut, J.; Mazzanti, M. *Chem. Sci.* **2012**, 3, 1075.

(5) (a) Skanthakumar, S.; Antonio, M. R.; Soderholm, L. A. *Inorg. Chem.* **2008**, *47*, 4591. (b) Almond, P. M.; Sykora, R. E.; Skanthakumar, S.; Soderholm, L.; Albrecht-Schmitt, T. E. *Inorg. Chem.* **2004**, *43*, 958. (c) Albrecht-Schmitt, T. E.; Almond, P. M.; Sykora, R. E. *Inorg. Chem.* **2003**, *42*, 3788. (d) Forbes, T. Z.; Wallace, C.; Burns, P. C. *Can. Mineral.* **2008**, *46*, 1623. (e) Forbes, T. Z.; Burns, P. C.; Skanthakumar, S.; Soderholm, L. *J. Am. Chem. Soc.* **2007**, *129*, 2760. (f) Wang, S.; Alekseev, E. V.; Depmeier, W.; Albrecht-Schmitt, T. E. *Inorg. Chem.* **2011**, *50*, 4692. (g) Sarsfield, M. J.; Taylor, R. J.; Maher, C. J. *Radiochim. Acta* **2007**, *95*, 677. (h) Forbes, T. Z.; Burns, P. C. *J. Solid State Chem.* **2007**, *180*, 106. (i) Almond, P. M.; Skanthakumar, S.; Soderholm, L.; Burns, P. C. *Chem. Mater.* **2007**, *19*, 280. (j) Jin, G. B.; Skanthakumar, S.; Soderholm, L. *Inorg. Chem.* **2011**, *50*, 6297. (k) Jin, G. B.; Skanthakumar, S.; Soderholm, L. *Inorg. Chem.* **2011**, *50*, 5203. (l) Forbes, T. Z.; Burns, P. C.; Soderholm, L.; Skanthakumar, S. *Chem. Mater.* **2006**, *18*, 1643. (m) Grigor'ev, M. S.; Baturin, N. A.; Budantseva, N. A.; Fedoseev, A. M. *Radiokhimiya* **1993**, *35*, 29. (n) Grigor'ev, M. S.; Baturin, N. A.; Fedoseev, A. M.; Budantseva, N. A. *Russ. J. Coord. Chem.* **1994**, *20*, 523.

(6) (a) Weng, Z.; Wang, S.; Ling, J.; Morrison, J. M.; Burns, P. C. *Inorg. Chem.* **2012**, *51*, 7185. (b) Mihalcea, I.; Henry, N.; Clavier, N.; Dacheux, N.; Loiseau, T. *Inorg. Chem.* **2011**, *50*, 6243. (c) Severance, R. C.; Smith, M. D.; zur Loye, H. *Inorg. Chem.* **2011**, *50*, 7931. (d) Lhoste, J.; Henry, N.; Roussel, P.; Loiseau, T.; Abraham, F. *Dalton Trans.* **2011**, *40*, 2422.

(7) (a) Alekseev, E. V.; Krivovichev, S. V.; Malcherek, T.; Depmeier, W. *Inorg. Chem.* **2007**, *46*, 8442. (b) Kubatko, K.; Burns, P. C. *Inorg. Chem.* **2006**, *45*, 10277. (c) Alekseev, E. V.; Krivovichev, S. V.; Depmeier, W.; Siidra, O. I.; Knorr, K.; Suleimanov, E. V.; Chuprunov, E. V. *Angew. Chem., Int. Ed.* **2006**, *45*, 7233. (d) Sullens, T. A.; Jensen, R. A.; Shvareva, T. Y.; Albrecht-Schmitt, T. E. *J. Am. Chem. Soc.* **2004**, *126*, 2676. (e) Alekseev, E. V.; Krivovichev, S. V.; Depmeier, W. *J. Solid State Chem.* **2009**, *182*, 2977. (f) Morrison, J. M.; Moore-Shay, L. J.; Burns, P. C. *Inorg. Chem.* **2001**, *50*, 2272.

(8) SADABS, Program for absorption correction using SMART CCD based on the method of Blessing; Sheldrick, G. M. *Acta Crystallogr.* **1995**, *A51*, 33.

(9) Sheldrick, G. M. *SHELXTL PC, An Integrated System for Solving, Refining, and Displaying Crystal Structures from Diffraction Data*, version 6.12; Siemens Analytical X-ray Instruments, Inc.: Madison, WI, 2001.

(10) (a) Burns, P. C.; Ewing, R. C.; Hawthorne, F. C. *Can. Mineral.* **1997**, *35*, 1551. (b) Brese, N. E.; O'Keeffe, M. *Acta Crystallogr.* **1991**, *B47*, 192.

(11) (a) Liu, G.; Beitz, J. V. In *The Chemistry of the Actinide and Transactinides Elements*; Morss, L. R., Edelstein, N. M., Fuger, J., Eds.; Springer: Heidelberg, Germany, 2006; p 2088.

(12) Adelani, P. O.; Albrecht-Schmitt, T. E. *Inorg. Chem.* **2010**, *49*, 5701.

(13) (a) Adelani, P. O.; Oliver, A. G.; Albrecht-Schmitt, T. E. *Inorg. Chem.* **2012**, *51*, 4885. (b) Adelani, P. O.; Albrecht-Schmitt, T. E. *Cryst. Growth Des.* **2011**, *11*, 4676. (c) Hardwick, H. C.; Royal, D. S.; Helliwell, M.; Pope, S. J. A.; Ashton, L.; Goodacre, R.; Sharrad, C. A. *Dalton Trans.* **2011**, *40*, 5939. (d) Adelani, P. O.; Albrecht-Schmitt, T. E. *J. Solid State Chem.* **2012**, *192*, 377.